Monomode Interband Cascade Lasers at 5.2 µm for Nitric Oxide Sensing

Michael von Edlinger, Julian Scheuermann, Robert Weih, Christian Zimmermann, Lars Nähle, Marc Fischer, Johannes Koeth, *Member, IEEE*, Sven Höfling, *Senior Member, IEEE,* and Martin Kamp

Abstract—We demonstrate application-grade monomode distributed feedback (DFB) laser devices with emission wavelength around 5.2 µm suitable for nitric oxide sensing. The devices are based on interband cascade laser material that enables continuous wave operation in the mid-infrared spectral region, when mounted on a standard thermoelectrically cooled TO-style header. With etched vertical sidewall DFB gratings as wavelength selective elements, signal to noise ratios around 30 dB and typical tuning ranges greater than 12 nm were achieved, making the devices suitable for applications based on tunable laser absorption spectroscopy.

Index Terms—Distributed feedback (DFB) laser, interband cascade laser (ICL), mid-infrared, nitric oxide (NO) sensing, semiconductor laser, tunable laser absorption spectroscopy (TLAS)

I. INTRODUCTION

MONOMODE laser sources are key components of modern gas analyzers based on tunable laser absorption spectroscopy (TLAS). A multitude of applications has been realized in the past using distributed feedback (DFB) laser based sensor systems from visible to far-infrared wavelength ranges. The mid-infrared wavelength region between 3 and 6 µm is of high interest for TLAS, since the fundamental absorption lines of numerous important gas species like methane, formaldehyde or nitric oxide (see Fig. 1) are located here [1], [2]. Quantum cascade lasers (QCLs) [3] and interband cascade lasers (ICLs) [4] can provide monomode continuous wave (CW) emission at room temperature in this wavelength range [5]-[7]. The IC material approach is

particularly advantageous, when low power consumption or driving currents are required [8], [9], which is, e. g., crucial for portable battery operated devices.

Nitric oxide (NO) is a gas species of particular interest in the context of its formation from the combustion of fossil fuels and its contribution to air pollution. It is also very important in medical and health-care applications, e.g., optical breath analyzers, since NO has been identified as related to asthma.
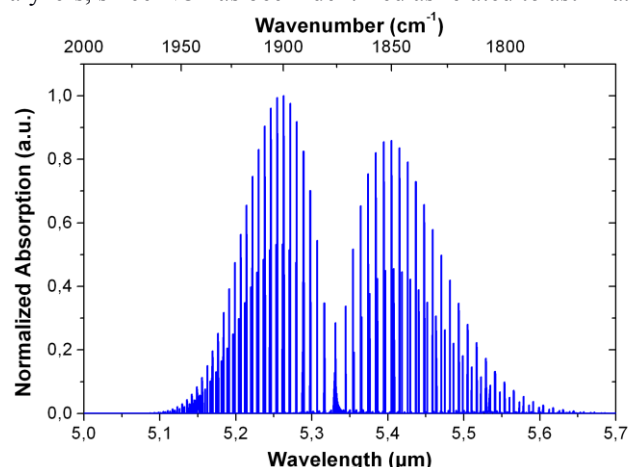

Fig. 1. Fundamental rotational-vibrational absorption features of nitric oxide located around 5.3 µm based on the HITRAN Database [2].

This work focuses on the manufacturing and the properties of application-grade monomode ICLs operating in CW mode around 5.2 µm, suitable for NO sensing applications.

II. GROWTH AND FABRICATION

The 5 stage ICL structure was grown by molecular beam epitaxy on a Te-doped GaSb substrate as described in [8], with some adaptations of the design to the longer emission wavelength: The thicknesses of the lower and upper AlSb/InAs superlattice claddings were chosen to 3.5 µm and 2 µm, respectively. In order to concentrate the optical mode in the 235 nm thick active region, two 380 nm high index GaSb separate confinement layers were inserted between cladding and active core. One cascade of the latter comprises the following layer sequence: 2.5 nm AlSb/2.4 nm InAs/3.0 nm $Ga_{0.65}In_{0.35}Sb$/1.9 nm InAs/1.0 nm AlSb/2.7 nm GaSb/1.0 nm AlSb/4.6 nm GaSb/2.5 nm AlSb/4.4 nm InAs/1.2 nm AlSb/3.0 nm InAs/1.2 nm AlSb/2.4 nm InAs. The band structure of this cascade is shown for an applied electric field of 80 kV/cm in Fig. 2, also the active W-quantum well (QW)

as well as the electron and hole injector regions are indicated. In addition, important probability densities of electrons and holes are shown.
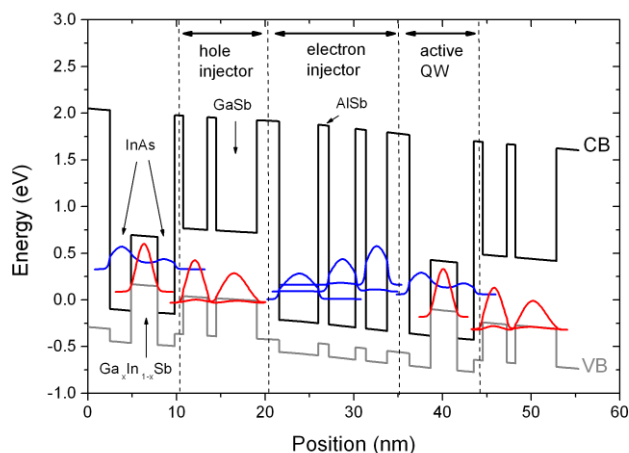

Fig. 2. Band structure and probability densities of important electron (blue) and hole (red) states in one cascade of the grown ICL structure under an electric field of 80 kV/cm. The injector regions and the active QW are indicated.

For rapid characterization of the grown structure, 100 µm wide, shallowly etched broad area (BA) devices were fabricated using optical contact lithography in combination with an inductive coupled plasma etch process. 2 mm long BA laser bars were cleaved off and characterized uncoated and unmounted under pulsed operating conditions.

For DFB fabrication on the grown ICL structure narrow ridges with fourth order vertical sidewall gratings were defined by electron beam lithography and dry etched into the bottom cladding layer with a chlorine/argon plasma based reactive ion etch (RIE) process. The grating period was varied around 3000 nm, while duty cycle and peak-to-valley amplitude were targeted at 37% and 1 µm, respectively. In Fig. 3 a scanning electron micrograph of a ridge waveguide structure with vertical sidewall gratings taken after the etching process is shown. The structures were passivated with a combination of Si_3N_4 and SiO_2 layers. Contact windows were opened on top of the ridges using CHF_3 based RIE. After sputter deposition of top contact metallization layers, the ridges were electroplated with thick (~10 µm) gold for improved heat removal.

The sample was cleaved into 900 µm long devices, which were coated with a high reflectivity Au mirror at the back facet and a thin Al_2O_3 passivation layer at the front facet. The devices were mounted epitaxial side up on Transistor Outline (TO) headers, which is an important industry standard and commonly used for electronic and optoelectronic packaging. The headers were sealed under dry N_2 atmosphere using suitable TO-cans. Attached to an adequate passive heat sink at room temperature, these thermoelectrically cooled devices allow laser chip operation temperatures down to -30 °C.
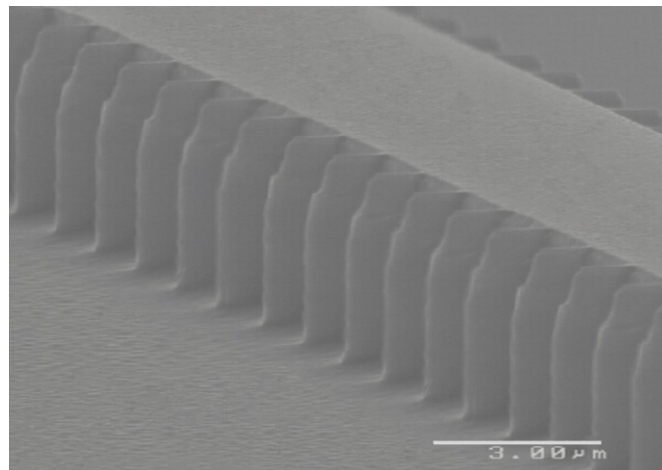

Fig. 3.   Scanning electron micrograph of an ICL DFB device during fabrication after RIE etching.

III. RESULTS

Pulsed measurements based on the BA laser devices show room temperature threshold current densities j_{th} and onset voltages U_0 of 760 A/cm^2 and 1.8 V, respectively. For the grown structure a theoretical minimum onset voltage $U_{0,ideal}$ of 1.2 V is calculated based on the number of stages and the corresponding photon energy, resulting in a voltage efficiency $U_{0,ideal}/U_0$ about 67%. The pulsed threshold power density of 1.37 kW/cm^2 is comparable to values of state of the art ICLs operating in the 5 µm wavelength range [10]. As we show within this work, application grade DFB laser devices are feasible based on this material in this wavelength range.

For application-grade laser devices a trade-off is required between output power on the one hand and power consumption as well as heat load on the other hand. Since TLAS typically only requires sub-mW-level of optical power, we focused on short narrow devices, reducing output powers for optimized power consumption.

The electro-optical characteristic at a chip temperature of -5°C of a fabricated DFB device with monomode CW laser operation from -25 °C to 0 °C is presented in Fig. 4. Within the dynamic range of the setup no side modes could be detected. The side mode suppression ratio is therefore higher than the noise floor of 30 dB (see inset in Fig. 4), whereas the observed spectral linewidth is limited by the spectral resolution of the FTIR spectrometer of 0.125 cm^{-1}. The device emits suitable output power for TLAS applications with a threshold power consumption of 138 mW at -5 °C. This is more than an order of magnitude lower than typical values observed for QCLs, which are in the range of 2-5 W [7].

The temperature and current tuning behavior of this device is shown in Fig. 5 together with the positions of characteristic absorption lines of nitric oxide. This device covers more than 12 nm, including several relevant NO absorption features, i.e. the $R_{1/2}(16)$, $R_{3/2}(16)$ and $R_{1/2}(17)$ transitions. Current and temperature tuning ratios of 0.15 nm/mA and 0.52 nm/K have been observed, respectively.
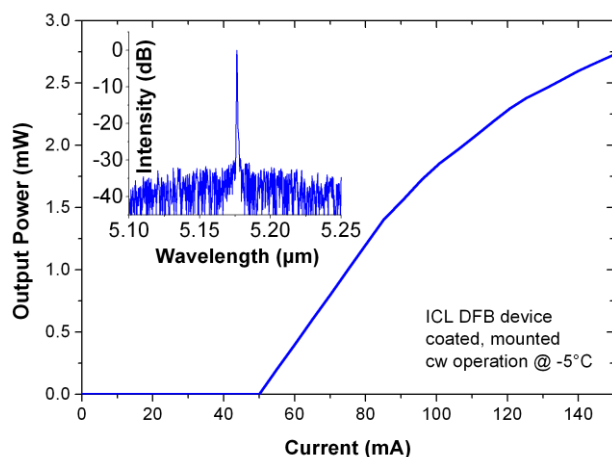
Fig. 4. Electro-optical characteristics and spectrum (inset) of an ICL DFB device mounted on TO-style header.

From the tuning behavior a thermal resistance-area product of 9.7 Kcm^2/kW was calculated. This is somewhat higher than reported for ICLs operating around 3.6 µm [11], mainly due to the thicker lower superlattice cladding with its poor thermal conductivity of 3 W/(m K) [12]. Calculations of the effective refractive index n_{eff} of the optical mode using the grating period Λ of 3000 nm and the Bragg condition $\lambda_{DFB}=2n_{eff}\Lambda/4$ for a fourth order grating yielded values for n_{eff} around 3.45 at -5 °C.
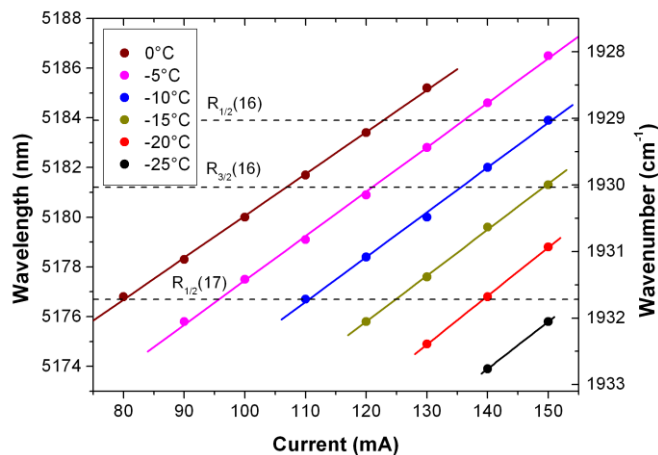

Fig. 5. Current and temperature dependent wavelength tuning characteristics of the device discussed in Figure 4. Dotted lines represent positions of important absorption features of nitric oxide.

Typically, CW operation based on these devices was observed up to 10 °C, whereas monomode emission could be maintained up to 5 °C. Thermal rollover was the limiting factor for maximum temperature and output power in all devices.

IV. CONCLUSION

We demonstrated application-grade DFB ICLs operating around 5.2 µm. Mounted on a standard TO-style header CW operation with suitable output power for an application in TLAS was achieved. By adapting the grating period we were able to successfully target NO absorption wavelengths. With signal to noise ratios of around 30 dB and tuning ranges greater than 12 nm, devices suitable for NO detection were realized.

REFERENCES

[1] S. Lundqvist, P Kluczinsky, R. Weih, M. v. Edlinger, L. Nähle, M. Fischer, A. Bauer, S. Höfling, J. Koeth, *Applied Optics*, Vol. 51, No. 25, 6009 (2012)
[2] http://hitran.iao.ru/ The HITRAN database, accessed 08 September 2013
[3] J. Faist, F. Capasso, D. Sivco, C. Sirtori, A. L. Hutchinson, A. Y. Cho, *Science*, Vol. 264, No. 5158, pp. 553-556 (1994)
[4] R. Yang, *Superlattices and Microstructures*, Vol. 17, No. 1, pp. 77-83 (1995)
[5] C. S. Kim, M. Kim, W. W. Bewley, J. R. Lindle, C. L. Canedy, J. Abell, I. Vurgaftman, J. R. Meyer, *Applied Physics Letters*, Vol. 95, Issue 23, 231103 (2009)
[6] S. Höfling, A. Bauer, R. Weih, M. Kamp, A. Forchel, *Proc. SPIE* 8432, 84320N (2012)
[7] Y. Yao, A. J. Hoffman, C. F. Gmachl, Nature Photonics 6, 432 (2012)
[8] G. Ryu,   A. N. Chryssis,   J. Amirloo,   S. Saini,   F .J. Towner, M. Dagenais, *Photonics Journal*, Vol. 4, No. 1, pp. 133-142 (2012)
[9] R. Weih, M. Kamp, S. Höfling, *Applied Physics Letters*, Vol. 102, Issue 23, 231123 (2013)
[10] W. W. Bewley, C. L. Canedy, C. S. Kim, M. Kim, C. D. Merrit, J. Abell, I. Vurgaftman, J. R. Meyer, *Optics Express*, Vol. 20, No. 3, 3235 (2012)
[11] W. W. Bewley, C. L. Canedy, C. S. Kim, M. Kim, C. D. Merrit, J. Abell, I. Vurgaftman, J. R. Meyer, *Optics Express*, Vol. 20, No. 19, 20894 (2012)
[12] T. Borca-Tasciuc, D. Achimov, W. L. Liu, G. Chen, H.-W. Ren, C.-H. Lin, S. S. Pei, *Microscale Thermophysical Engineering*, Vol. 5, No. 3, 225 (2001)